  Bull. Chem. Soc. Jpn., 60, 1985—1992 (1987)

Atropisomerism of Zinc Tetrakis(*o*-cyanophenyl)porphyrins. The Crystal Structure of the $\alpha\beta\alpha\beta$-Isomer and the Atropisomerization Rates

Keiichiro HATANO,* Kyoko KAWASAKI, Sonono MUNAKATA, and Yoichi IITAKA†
Department of Pharmaceutical Sciences, Nagoya City University, Mizuho-ku, Nagoya 467
†Faculty of Pharmaceutical Sciences, The University of Tokyo, Bunkyo-ku, Tokyo 113
(Received December 3, 1986)

The structure of one of the four atropisomers of tetrakis(*o*-cyanophenyl)porphyrin has been determined as the zinc complex by X-ray crystallographic methods. The five-coordinate zinc porphyrin with pyridine as the axial ligand also has a pyridine solvate in the crystal lattice. The conformation of the *o*-cyanophenyl rings is $\alpha\beta\alpha\beta$ as predicted previously. The two nitrogen atoms of the CN groups on the same side of the coordinated pyridine have close *intramolecular* contacts to pyridine at the van der Waals distance. However, the structural parameters, bond distances and angles of this molecule do not indicate distinct steric effects of the CN groups. Thermal atropisomerization among the four zinc porphyrin atropisomers occurs in solution. The quantitative composition of the atropisomers at equilibrium and the rates of the isomerization reaction have been determined with aliquots separated by TLC. A nonstatistical equilibrium distribution of the atropisomers suggests some mutual interactions among the CN groups. The slower isomerization rates of the zinc complexes compared to those of the free base have been discussed in connection with the molecular structure.

The synthetic model study has been one of the most powerful approaches in probing the relationship between function and structure of the prosthetic heme group in multifunctional hemoproteins. The fundamental functions of hemes such as ligand binding and electronic state changes of the central iron are controlled by various factors including the electronic and steric effects of substituents of the porphyrin periphery. In recent years, the subtle control of the electronic properties of hemes has been investigated by means of a wide and systematic variation of the porphyrin peripheral substitution.[1-3] Steric control of the functions of hemes and metalloporphyrins is an interesting subject in the model studies considering the role of proteins. A typical steric control of oxygen binding to heme models has been accomplished notably as the "picket fence" porphyrin in which the role of the bulky pivaloylamino substituents on the one side of the porphyrin plane is attributed to the appropriate pocket for dioxygen binding and the hindrance for dimer formation.[4] However, there have been few studies to evaluate the steric effects quantitatively using a systematic variation of substituents and so on.[4d,5-7] We have been interested in the four atropisomers of *o*-substituted tetraarylporphyrin since there is a possibility in designing three dimensional models using the steric effect of the substituents under the isoelectronic conditions to control the functions of metalloporphyrin molecules. On this line, we have reported some properties of the tetrakis (*o*-substitutedphenyl)porphyrin atropisomers, i.e., electronic spectra, redox potential and metal incorporation rates, rotational rate of phenyl rings, and axial coordination reactions of bases.[7,8] The molecular structure determination of porphyrin atropisomers is expected to offer essential information as to the steric effects and the stereochemical environment around the porphyrin.

On the other hand, there is some ambiguity in the assignment of the conformation of $\alpha\beta\alpha\beta$- and $\alpha\alpha\beta\beta$-isomers of 5,10,15,20-tetrakis(*o*-cyanophenyl)porphyrin(ToCNPP[9]) free bases because of small difference in TLC separation and nonstatistical equilibrium population of these isomers.[8a] The present X-ray crystal structure determination originally aimed to establish the conformation of the $\alpha\beta\alpha\beta$-form and, subsequently, all conformations of the four atropisomers of ToCNPP. However, the ToCNPP free bases are thermally unstable and isomerize under the ambient recrystallization conditions. The coordination of metal ions to the porphyrin has been predicted to retard the rotational isomerization rate of the substituted phenyl rings.[10] Thus, the metallation of the porphyrin is expected to make it possible to isolate a pure isomer. At the same time, we are interested in the effect of the coordination of metal ions on the isomerization rate, its relationship to the structure of porphyrin, and the effect of axial ligands of the metal ion on the atropisomerization. Herein we report the X-ray structural analysis of the $\alpha\beta\alpha\beta$-isomer of ZnToCNPP and the atropisomerization rates among the isomers.

Experimental

Synthesis and Isolation of Atropisomers of ZnToCNPP. All reagents and solvents were reagent grade and used without further purification. ToCNPP was prepared as described.[8a] Metallation of ToCNPP was performed by refluxing zinc acetate and a mixture of the four atropisomers in DMF. The completion of the reaction was checked by UV-visible spectra recorded on a Shimadzu 200-S spectrophotometer. The products were precipitated by pouring an excess of water into the reaction mixture and were collected by filtration. The metallated porphyrins, ZnToCNPP, were separated by TLC (Merck; eluting solvent, 5:95 ether-

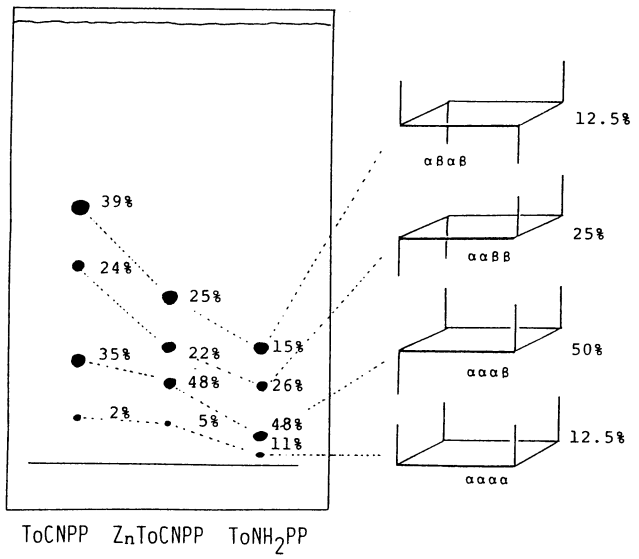

Fig. 1. The separation of atropisomers by thin layer chromatography and the distribution percentage of the isomers at the equilibrium. On the right the schematic representation of the assignment of four atropisomers and the statistical distribution are shown.

$CHCl_3$). The resolution of the four atropisomers is shown in Fig. 1 along with those of the corresponding ToCNPP and $ToNH_2PP$. The isolation of the respective atropisomers was accomplished by column chromatography on silica gel eluted with 98:2 chloroform-ether. The fractions of each isomer were evaporated to dryness immediately after elution from the column to avoid atropisomerization. The purity of each isomer was found to be more than 85%, satisfactory for the following kinetic experiments. Only the $\alpha\beta\alpha\beta$-isomer was purified further by recrystallization from chloroform-methanol, yielding purple crystals. Anal. Calcd for Zn(ToCNPP) $CHCl_3$, $C_{49}H_{25}N_8Cl_3Zn$: C, 65.57; H, 2.81; N, 12.48%. Found: C, 65.58; H, 2.51; N, 12.52%.

Crystal Structure Determination. Single crystals suitable for X-ray diffraction were obtained by vapor diffusion of pentane into a pyridine solution of the $\alpha\beta\alpha\beta$-isomer of ZnToCNPP. Crystals of $\alpha\beta\alpha\beta$-ZnToCNPP(Py)·Py were examined on a Philips PW-1100 automated diffractometer. This established a four-molecule monoclinic unit cell with *Cc* or *C2/c* as the possible space group. Least-squares refinement of the setting angles of 25 reflections gave the cell constants reported in Table 1. Table 1 also reports other details of crystal data and intensity collection. Intensity data were reduced to the structure factors without absorption corrections.

The choice of *C2/c* as the space group requires that the molecule possess a two-fold axis passing through Zn in porphyrin plane or an inversion center on Zn. However, the probable zinc locations calculated from the Patterson map lead to featureless difference Fourier maps and the Patterson map itself was incompatible with a crystallographic two-fold axis passing through the center of the tetragonal porphyrin molecule.[11] Thus, the *Cc* space group was chosen and all subsequent developments of the structure analysis of the complex were consistent with this choice.

A series of difference Fourier syntheses, phased initially by the zinc atom, revealed all non-hydrogen atoms of the porphyrin framework and a coordinated pyridine. After several cycles of refinement using these atoms, a difference Fourier map revealed six atomic positions of a solvate pyridine and several hydrogen positions of the porphyrin skeleton. The solvated pyridine was refined by assuming it as benzene i.e., six carbon atoms. All hydrogen atoms of the porphyrin and coordinated pyridine were idealized with C-H=0.95 Å and assigned isotropic temperature factors one unit higher than the associated atom. Refinement was then carried to convergence with anisotropic temperature factors for all non-hydrogen atoms using the block-diagonal least-squares and two-block 'full matrix' least-squares method.[11] At covergence, the final R and R_w values were 0.053 and 0.051, respectively. Calculations for the opposite enantiomorph gave R=0.059 and R_w=0.061. The coordinates of the first choice are reported. A final difference Fourier synthesis was featureless (<0.48 e/Å^3). A listing of observed and calculated structure factors is available as supplementary material (Table S1[12]). Tables 2 and S2[12] list final atomic coordinates with isotropic equivalent temperature factors and the associated anisotropic temperature factors, respectively.

Table 1. Summary of Crystal Data and Intensity-Collection Parameters for ZnToCNPP(Py)·Py

Formula	$ZnC_{58}H_{34}N_{10}$
F.W., amu	936.4
Crystal dimensions	0.3×0.3×0.7 mm^3
Space group	*Cc*
Temperature	293 K
a, Å	18.805(2)
b, Å	16.647(4)
c, Å	16.724(2)
β, °	115.49(12)
V, Å^3	4725.6
Z	4
Calcd density	1.316 g cm^{-3}
Obsd density	1.314 g cm^{-3}
2 theta range	6—54°
Criterion for observation	$F_o>2\sigma(F_o)$
Unique obsd data	3898
R	0.053
R_w	0.051
Data/Parameters	6.3

Atropisomerization. A toluene or 1,1,2-trichloroethane solution of each isolated isomer (ca. 5 mg/20 ml) in a flask was placed in a heated oil bath. Aliquots sampled by a glass capillary were spotted at intervals on TLC and developed with 95:5 $CHCl_3$-ether. The separated isomers were extracted two times with $CHCl_3$ and diluted to a constant volume in a cuvette. The quantity of the four isomers was analyzed by the spectrometric absorption area in the 390—450 nm region and was normalized to a molecular ratio of four atropisomers. The rates of isomerization were determined by a combination of the Runge-Kutta simulation and least-squares curve-fitting techniques.[8]

Results and Discussion

Molecular Structure of $\alpha\beta\alpha\beta$-Zn(ToCNPP)(Py). The structure of the ZnToCNPP(Py) molecule is shown in two different orientations in Figs. 2 and 3,

Table 2. The Fractional Coordinates and Isotropic Equivalent Temperature Factors

Atom	x	y	z	B_{eq}	Atom	x	y	z	B_{eq}
Zn	1/2	0.3632(0)	1/4	4.3	C5	0.3461(4)	0.5763(5)	0.5059(5)	7.8
NP1	0.6120(3)	0.3597(3)	0.3644(3)	4.8	C6	0.3848(4)	0.5418(5)	0.4617(5)	6.8
N1	0.4689(2)	0.4824(3)	0.2530(3)	4.3	C7	0.3905(3)	0.1059(4)	0.2978(4)	5.1
N2	0.4172(3)	0.3314(3)	0.2949(3)	4.6	C8	0.4441(4)	0.0549(3)	0.3624(4)	5.1
N3	0.4951(3)	0.2464(3)	0.2054(3)	4.9	C9	0.4207(4)	−0.0186(4)	0.3838(5)	6.8
N4	0.5466(3)	0.3979(3)	0.1619(3)	4.6	C10	0.3425(5)	−0.0402(4)	0.3389(6)	8.5
CP1	0.6576(4)	0.2959(4)	0.3839(5)	7.4	C11	0.2887(4)	0.0107(5)	0.2779(5)	7.3
CP2	0.7347(5)	0.2976(5)	0.4484(7)	9.2	C12	0.3131(4)	0.0817(4)	0.2569(5)	6.0
CP3	0.7636(4)	0.3635(5)	0.4949(6)	8.5	C13	0.5677(3)	0.6217(3)	0.1536(4)	5.0
CP4	0.7175(4)	0.4337(5)	0.4753(5)	7.4	C14	0.5393(4)	0.6476(4)	0.0661(5)	6.1
CP5	0.6434(4)	0.4290(4)	0.4091(4)	5.9	C15	0.5652(4)	0.7207(4)	0.0447(5)	7.1
CA1	0.4952(3)	0.5472(3)	0.2232(4)	4.4	C16	0.6198(4)	0.7678(4)	0.1116(5)	7.6
CA2	0.4251(3)	0.5117(3)	0.2940(4)	5.0	C17	0.6467(4)	0.7451(4)	0.1984(5)	6.7
CA3	0.3839(3)	0.3816(3)	0.3337(4)	4.6	C18	0.6217(4)	0.6724(4)	0.2208(4)	5.2
CA4	0.3975(3)	0.2541(3)	0.3084(4)	4.6	C19	0.6100(4)	0.2192(4)	0.0694(5)	6.6
CA5	0.5332(3)	0.2174(3)	0.1583(4)	5.7	C20	0.5668(4)	0.2013(4)	−0.0172(5)	7.3
CA6	0.4629(3)	0.1805(3)	0.2287(4)	4.6	C21	0.6030(6)	0.1584(5)	−0.0654(6)	10.5
CA7	0.5645(3)	0.4737(3)	0.1472(4)	4.3	C22	0.6818(6)	0.1337(5)	−0.0176(8)	12.6
CA8	0.5770(3)	0.3476(3)	0.1203(4)	4.9	C23	0.7230(5)	0.1505(6)	0.0680(7)	10.8
CB1	0.4646(4)	0.6196(3)	0.2442(5)	6.2	C24	0.6889(5)	0.1942(5)	0.1133(6)	9.5
CB2	0.4213(4)	0.5993(4)	0.2872(5)	5.8	CN1	0.2179(4)	0.4889(4)	0.2506(5)	6.6
CB3	0.3448(4)	0.3338(4)	0.3756(4)	5.8	NC1	0.1791(4)	0.4666(5)	0.1773(5)	10.1
CB4	0.3538(3)	0.2572(4)	0.3604(4)	5.3	CN2	0.5238(4)	0.0802(4)	0.4083(5)	5.7
CB5	0.5256(4)	0.1303(4)	0.1516(4)	6.0	NC2	0.5868(3)	0.1004(4)	0.4462(4)	7.5
CB6	0.4808(4)	0.1091(3)	0.1934(4)	5.5	CN3	0.6519(4)	0.6492(4)	0.3107(5)	6.0
CB7	0.6083(4)	0.4718(4)	0.0953(4)	5.9	NC3	0.6783(4)	0.6313(4)	0.3839(4)	8.3
CB8	0.6142(4)	0.3934(4)	0.0760(4)	5.8	CN4	0.4858(5)	0.2221(4)	−0.0608(5)	7.2
CM1	0.3872(3)	0.4648(3)	0.3338(4)	4.7	NC4	0.4196(4)	0.2359(4)	−0.0935(5)	8.6
CM2	0.4179(3)	0.1842(3)	0.2767(4)	4.5	NP2	−0.0383(5)	0.3485(6)	0.2219(6)	9.1
CM3	0.5421(3)	0.5441(3)	0.1765(4)	4.6	CP6	−0.0050(6)	0.3861(6)	0.1729(7)	11.0
CM4	0.5724(4)	0.2631(4)	0.1202(4)	5.6	CP7	−0.0405(6)	0.4081(6)	0.0909(6)	10.6
C1	0.3441(3)	0.5099(3)	0.3772(4)	5.2	CP8	−0.1207(6)	0.3993(6)	0.0436(7)	11.5
C2	0.2622(3)	0.5184(3)	0.3357(4)	5.0	CP9	−0.1593(6)	0.3564(7)	0.0879(9)	13.6
C3	0.2237(4)	0.5549(4)	0.3816(5)	6.6	CP10	−0.1171(6)	0.3368(7)	0.1788(8)	13.3
C4	0.2657(4)	0.5807(5)	0.4672(6)	8.7					

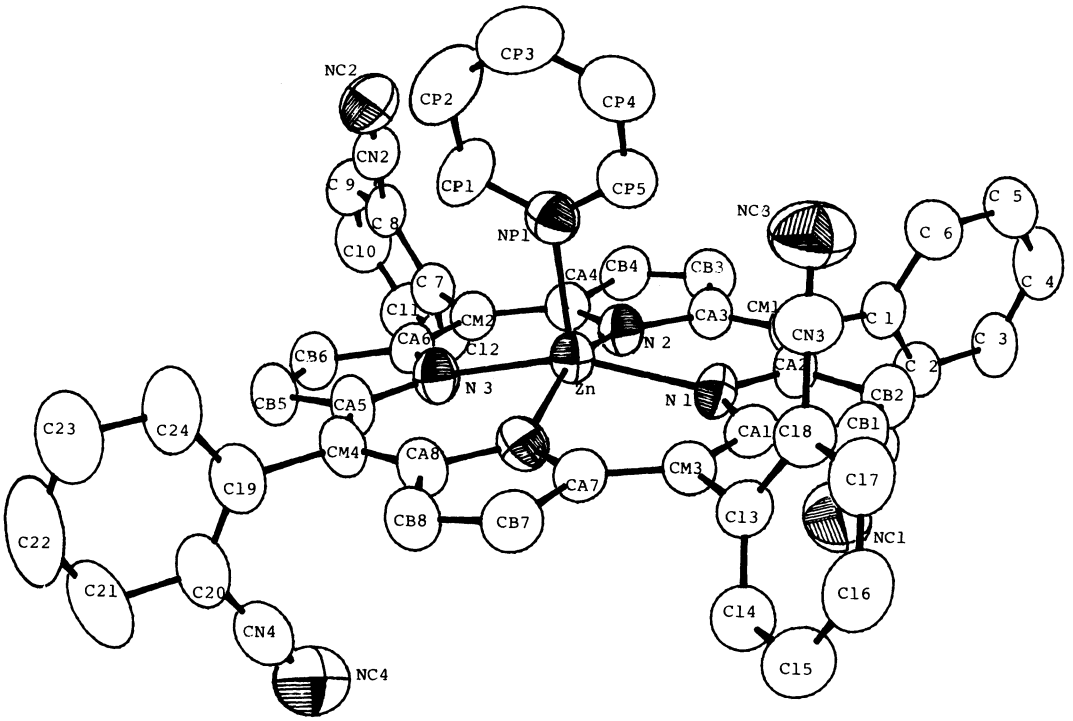

Fig. 2. Computer-drawn model of the ZnToCNPP(Py) molecule. The labeling scheme for the atoms is given. Zinc and nitrogen atoms are shown by the octant shading ellipsoids. Ellipsoids are contoured to enclose 50% of the electron density.

Table 3. Average Values of Bond Distances and Angles of the Porphyrin Skeleton in ZnToCNPP(Py)·Py

		Bond Distance/Å			
$Zn-N_{por}$	2.076(12)	$N_{por}-Ca$	1.369(11)	Ca–Cb	1.444(13)
Cb–Cb	1.347(14)	Ca–Cm	1.398(8)		
		Bond Angle/deg.			
$Zn-N_{por}-Ca$		126.2(5)	$N_{por}-Ca-Cb$		109.5(4)
$Ca-N_{por}-Ca$		106.8(4)	$N_{por}-Ca-Cm$		125.4(4)
Ca–Cm–Ca		125.9(4)	Ca–Cb–Cb		107.1(9)

Ca, Cb, and Cm denote atoms of pyrrole-α, pyrrole-β, and methine(5,10,15,20-) positions of porphyrin skeleton, respectively.

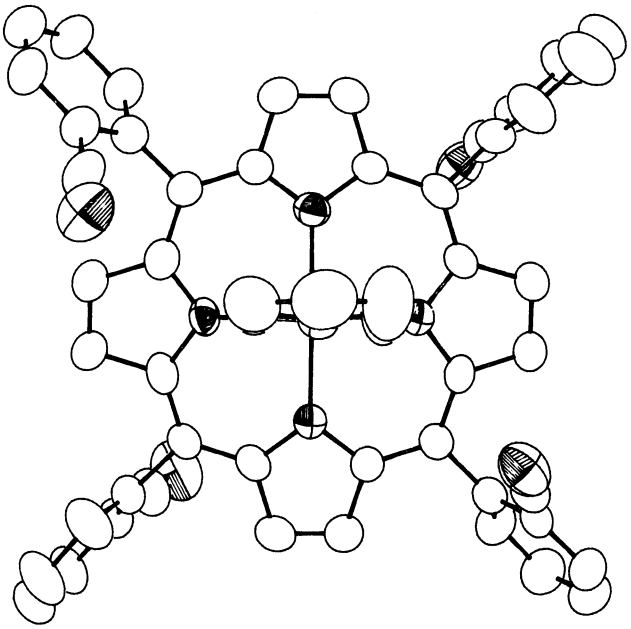

Fig. 3. Perspective view of the ZnToCNPP(Py) molecule looking down the nomal of the porphyrin plane, showing the relative orientation of coordinating pyridine and geometry of the CN groups.

which demonstrate the most significant feature of the molecule: The arrangement of the CN groups and nonbonded intramolecular contacts between the CN group and the coordinated pyridine. Figure 2 also gives the labels assigned to each non-hydrogen atom. The structure is in agreement with the conformation ($\alpha\beta\alpha\beta$) of the atropisomer identified previously by chemical properties and chromatographic separation, i.e., the atropisomer eluting most rapidly on silica gel and consequently being least polar.

Average values for the chemically equivalent bond lengths and angles of the porphinato core are given in Table 3. The numbers in parentheses are the standard deviations calculated from the differences between the average of the equivalent bonds and the individual values (Table S3[12]).[13]

The coordination state of the present zinc porphyrin is five-coordinate with a pyridine molecule in the fifth axial position. The coordination sphere around Zn is apparently normal. The average $Zn-N_{por}$ bond length of 2.076 (12) Å and the displacement (0.37 Å) of the zinc ion out of the mean plane of the four porphinato N atoms are in general accord with those observed in the five-coordinate zinc porphyrins as shown in Table 4. The $Zn-N_{py}$ bond length of 2.151 (4) Å does not display any elongation due to a steric effect between the pyridine and the two CN substituents projecting toward pyridine. Indeed the bond length is significantly shorter (by 0.049 Å) than the 2.200 (3) Å value reported for Zn(OEP)(Py)[14] which has no hindering substituents on the porphyrin periphery. This indicates that the CN substituents on the ortho position in the $\alpha\beta\alpha\beta$ phenyl conformation have little steric effect on the coordinated pyridine molecule, or, even if there is any, the effect is not necessarily hindering or repulsive.

The dihedral angle between the axial pyridine plane and the plane containing three nitrogen atoms, those of pyridine and two opposite pyrroles of the porphyrin core, is small at 8.8°. The actual ligand orientation

Table 4. Comparison of the Stereochemical Parameters of the Coordination Group for Five-Coordinate Zinc Porphyrins

Zn Porphyrin	Distance/Å			ϕ/°	Ref.
	$Zn-N_{por}$	$Zn-N_{Py}$	Zn–Ct		
$ZnTPP(H_2O)$	2.05	2.20*	0.19	—	(15)
ZnTPyP(Py)	2.073(3)	2.143(4)	0.33	23	(16)
ZnOEP(Py)	2.067(3)	2.200(3)	0.31	4	(14)
Zn(TPP side arm Py)	2.059(7)	2.147(7)	0.37	5.8	(17)
ZnToCNPP	2.076(12)	2.151(4)	0.37	8.9	This work

* $Zn-O_{water}$ distance.

would appear to have ϕ[18] closer to a completely eclipsed conformation (i.e. ϕ=0°); the apparent value of 8.8° results in part from the pyridine plane not being precisely perpendicular to the 24-atom porphinato plane, the angle is 77.0°. As reported in Table 4, the ligand orientation of five-coordinate zinc porphyrins have, in general, small values. This means that sterically unfavoring contacts between α-hydrogen of pyridine and porphinato pyrrole nitrogen result if no other constraint controls the orientation. Although the constraint of the side arm has been explained to lead to an exceptionally small ϕ value of Zn(TPP side arm Py),[17] the present structure indicates no distinct evidence that the orientation of the ligand is controlled by the CN substituents. The closest contact of N_{CN} to non-hydrogen atoms of the coordinated pyridine is 3.49 Å (NC2-CP2), which is a normal van der Waals contact. Even if there would be a closer contact, it can be circumvented by the small rotation about the aryl-porphine bond. There is a considerable room for the rotation since the dihedral angles between cyanophenyl rings and the mean porphyrin plane are 73.3° and 64.7° on the pyridine side and 77.9° and 87.8° on the other side.

Recently, Scheidt et al. suggest that the electronic spin-state is one of the important factors correlating with ligand orientation in some iron(III) porphyrin cases.[19] The zinc ion has a d^{10} electronic configuration and all five 3d orbitals are occupied by spin-paired electrons, hence, the drastic changes in the electronic states or spin states depending implicitly on the change of axial ligands, bond lengths, or ligand orientation are *not* expected for zinc porphyrins. Consequently, the small orientation angle observed in all of the pyridine-ligated zinc porphyrins reported so far should be explained by an intrinsic electronic nature of zinc(II) ion. A possible explanation comes from consideration of the overlap of the occupied d_{zx} or d_{yz} orbital over pπ* at the N_{Py} atom, namely dπ-pπ* backdonation, because the d_{zx} or d_{yz} has a common nodal plane with pπ* at ϕ=0°.

The structural similarity of six- and five-coordinate porphyrin complexes of zinc(II) and high-spin iron(II) has been pointed out by Schauer et al.[20] The similarity includes the bond distances between the metal ion and porphinato nitrogen atoms and the axial N_{base}-metal bond length. The structural similarity can also extend to five-coordinate high-spin iron(III) complexes since a novel structure of five-coordinate [Fe(OEP)(2Mim)]ClO_4 molecule has been determined recently.[21] The structural parameters, 2.038(6) Å for average Fe-N_{por}, 2.068(4) Å for Fe-N_{2Mim}, and 0.35 Å for displacement of Fe(III) out of plane, are comparable to those of five-coordinate zinc porphyrins in Table 4. Here, a small orientational angle (ϕ=3.0—7.3°) of the 2-methylimidazole ligand can be particularly emphasized as part of the similarity. This suggests that the occupation of electrons in all of the five 3d orbitals has an essential and common effect on the coordination structure in porphyrin complexes of these two metal ions.

The structure of four peripheral cyanophenyl groups shows no abnormal feature in the bond distances and angles irrespective of whether the CN substituents are on the same side as the coordinated pyridine or not. The CN group is coplanar to each phenyl ring within 0.07 Å from the mean plane. Figure 4 shows the average bond parameters for the four chemically equivalent types with the standard deviations in parentheses. The average C-C_{CN} bond length is 1.411(13) Å, similar to the C-C bonds of the phenyl ring. Thus, the bond has a conjugated double bond character. The C≡N distance ranges from 1.128(8) Å to 1.184(9) Å and the average is 1.151(24) Å. These bond values agree well with those of benzonitrile or cyanomethanide ion disregarding whether the molecule or ion is free or coordinated to a metal.[22,23]

The nonbonded intramolecular N_{CN}-N_{CN} atomic distances are measured to be 9.15 Å at a level 3.2 Å above the porphyrin plane on the pyridine side and 8.56 Å at a level 3.4 Å below the plane on the other side. These distances correspond to a diameter of the cavity defined by the CN substituents. The diameter is comparable with the interior size of some inclusion compounds, e.g., ca. 8.5 Å for cyclohexaamyloses or ca. 8.6 Å for cyclophanes.[24,25] We have noted previously that the free base atropisomers (ToCNPP) populate in a nonstatistical equilibrium ratio (cf. Fig. 1) because of the mutual nonbonded interaction of the CN substituents on the same side of the porphyrin plane. A similar nonstatistical distribution is also observed in ZnToCNPP. The rather large diameter of the cavity requires the idea of the nonbonded tran-

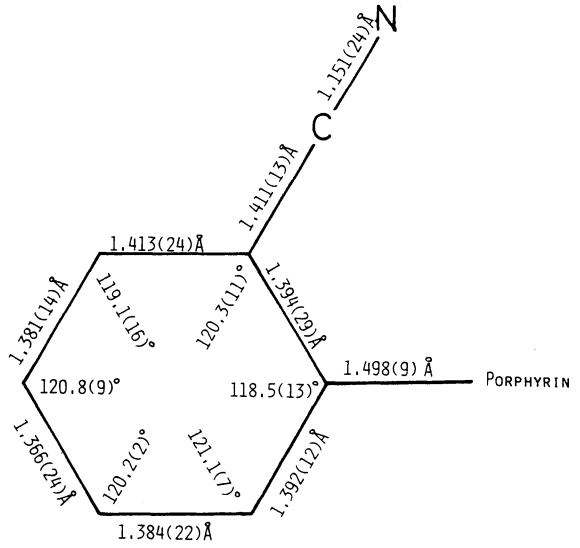

Fig. 4. A formal diagram of the average structure of four cyanophenyl rings of the molecule. Average values of bond distances and angles are displayed with the standard deviations[13] of the least significant digits in parentheses.

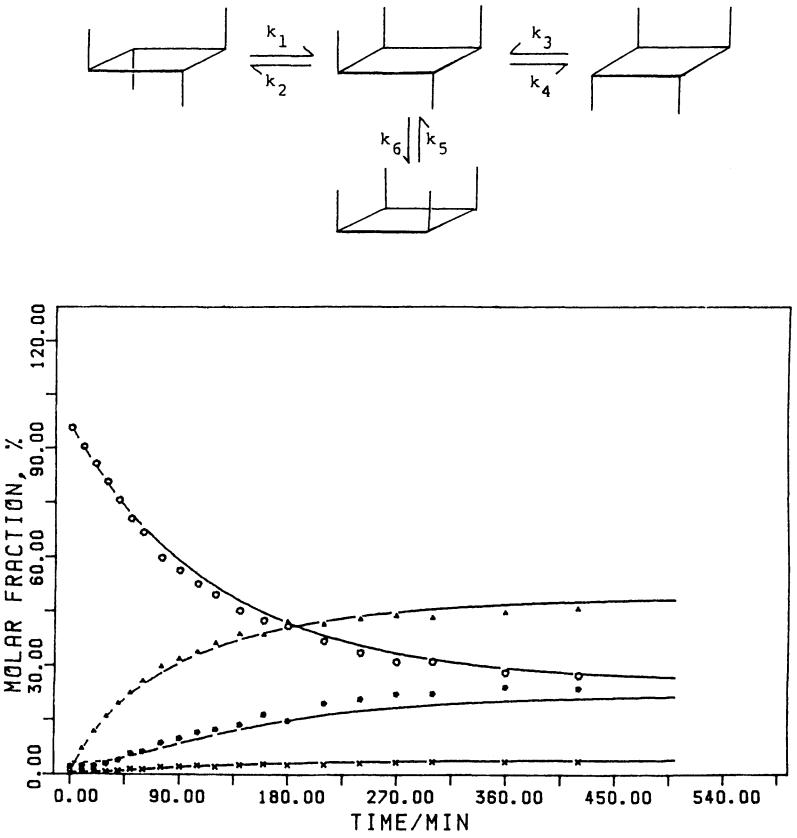

Fig. 5. The reaction scheme of the atropisomerization and a time course diagram of the reactions initiating from $\alpha\beta\alpha\beta$-isomer of ZnToCNPP at 96 °C, (○) $\alpha\beta\alpha\beta$; (●) $\alpha\alpha\beta\beta$; (▲) $\alpha\alpha\alpha\beta$; (×) $\alpha\alpha\alpha\alpha$. The solid lines in the diagram were computed by the Runge-Kutta method from the rate constants in Table 5.

sannular interaction to be not necessarily direct but maybe indirect through axial ligands or solvents in the vicinity of the cavity.

The maximum displacement from the 24-atom mean porphyrin plane is as small as 0.16 Å of the CB2 atom, namely, the porphyrin skeleton is fairly planar for ZnToCNPP. Although there seems to be no clear-cut general interpretation as to whether the porphyrin takes planar or "ruffled" skeleton depending on the metal ions and so on, the zinc coordination has a trend in favor of the planar structure. The planar structure of the porphyrin core may correlate with the inflexibility of the core for the deformation required in the transition state of the atropisomerization reaction as discussed below.

Atropisomerization of ZnToCNPP. Figure 5 depicts schematic isomerization reactions among the atropisomers along with the definition of rate constants and a typical result of kinetic experiments. The relative ratio of the amount of four atropisomers equilibrating at 96 °C for 2 d was as follows: $\alpha\alpha\alpha\alpha$,5 (2); $\alpha\alpha\beta\beta$, 48 (4); $\alpha\alpha\beta\beta$, 22 (4); $\alpha\beta\alpha\beta$, 25 (3). The ratio was found to be independent of temperatures in the range of 75° to 105 °C within the experimental deviations in parentheses. The individual reaction rates were investigated in several independent runs at 65, 75, 85, 96, and 105 °C. The observed average rate constants are listed in Table 5. Considering the constant population of the isomers in the equilibrium at any temperature in our experiments, we analyzed the rates by obtaining first the average Arrhenius activation energy (E_a) and then individual preexponential terms for six rate constants using the least-squares method. This treatment demands a constant ratio in the six rate constants at any temperature. The ratio is $1:0.51:2.9:1.3:5.3:0.46$ for $k_1:k_2:k_3:k_4:k_5:k_6$. The thermodynamic parameters could be obtained by the use of relation-

Table 5. Observed Rate Constants for Atropisomerization Reactions of Tetrakis(*o*-cyanophenyl)-porphinatozinc(II)

Temperature	Observed Rate Constant ($\times 10^5$)/s^{-1}					
°C	k_1	k_2	k_3	k_4	k_5	k_6
65	0.50	0.27	1.42	0.75	2.65	0.22
75	1.15	0.58	3.85	1.65	6.35	0.64
85	3.35	1.60	9.20	4.15	16.5	1.60
96	10.5	5.5	26.5	11.5	53.5	4.5
105	21.0	11.0	65.0	30.0	115.0	8.5

Table 6. Comparative Activation Parameters for the Atropiosomerization Rate (k_1)

Porphyrin	Temperature	ΔH^*	ΔS^*	ΔG^*[a]	Ref.
	°C	(kJ mol^{-1})	(JK^{-1} mol^{-1})	(kJ mol^{-1})	
ZnToCNPP	85	97.6	−59.5	118.9	This work
	65	97.6	−59.9	117.7	This work
ToCNPP	60	85.8	−68.2	108.4	(8a)
ToNH_2PP	65	91.3	−61.5	112.2	(8b)

a) Extrapolated values.

ships, $\Delta H^*=E_a-RT$ and $\Delta G^*=\Delta H^*-T\Delta S^*$, and the Eyring equation, $k=(k_BT/h)\exp(-\Delta G^*/k_BT)$. The values for the one representative reaction (k_1) are shown in Table 6. The kinetic data processed as above were consistent with all of the observed rate constants within the experimental errors. The activation parameters calculated similarly for the same reaction (k_1) of ToCNPP[8a] and ToNH_2PP[8b] are also shown in Table 6 for comparison.

The slower rates of ZnToCNPP relative to those of ToCNPP are remarkable. The ΔG^* value of 118.9 kJ mol^{-1} at 85 °C is high and comparable to the 113.1 kJ mol^{-1} value at 81 °C reported for the bulky hexadecyl derivative of ToNH_2PP.[26] The phenyl ring rotation in *o*-substituted tetraarylporphyrins is thought to require the severe deformation of the porphyrin skeleton. The slow rates of the Zn complex suggest that the zinc ion coordination (perhaps metal ion coordination in general) brings a reinforcement of the skeletal tension against the required deformation. The higher free energy of activation of ZnToCNPP, consequently the slower rate, compared to that of ToCNPP at 60 or 65 °C also reflect the reinforcement as the part of the stabilization energy of the porphyrin acquired by the incorporation of the zinc ion. The reinforcement effect seems to correlate with the enthalpy term of the free energy of activation because of the identical entropy values obtained from the reactions of ZnToCNPP and ToCNPP (Table 6). This is contrasting with the entropy control of activation observed in a series of the free base porphyrins with bulky *o*-substituents.[8b]

The retardation factor of the isomerization reaction induced by the coordination of zinc reaches about 20 at 60 °C and the factor is appreciably larger than the apparent value of 12.5 calculated from the data for the ToOHPP-Cu system.[10] The difference in the retardation factor may come from the difference in the porphyrin core expansion by the two metal ions. In this connection, the bond length between the metal and the porphyrin nitrogen can be cited as 1.981 Å for CuTPP[27] and 2.036 Å for ZnTPP:[28] both metalloporphyrins are four-coordinate; CuTPP is ruffled whereas ZnTPP is planar.[29] Thus, the coordination of zinc ion is thought to bring forth not simply the reinforcement against deformation but also to some extent as expansion effect on the porphyrin skeleton. The expansion of porphyrin core should weaken the transannular interaction among *o*-substituents on the same side of the porphyrin plane. This may be a possible explanation for why the equilibrium distribution of atropisomers of ZnToCNPP becomes closer to the statistical ratio than that of metal-free ToCNPP. We have speculated that the nonbonded distance between two adjacent nitrogen atoms of CN group is responsible for the nonstatistical isomer distribution.[8a] However, the transannular interaction occur not always through the directly measured *intramolecular* distance since short *intermolecular* contacts such as van der Waals distance are frequently observed in the solid state. In solution, the intramolecular transannular interaction must be affected by the solvent molecule therein, especially the coordinating impurities in the case of metalloporphyrin. The present five-coordinate ZnToCNPP structure demonstrate a possibility of some interaction through the coordinated pyridine by the shortest contact of 3.49 Å with the CN substituent as mentioned above. The addition of pyridine as an effector into the reaction solution did not give distinct changes in the equilibrium distribution of isomers. A drastic change was observed in the presence of some other particular molecules such as 2Mim[9] in the reaction mixture. The observed distribution in the presence of 2Mim is as follows: $\alpha\alpha\alpha\alpha$, 15(3); $\alpha\alpha\alpha\beta$, 52(5); $\alpha\alpha\beta\beta$, 19(4); $\alpha\beta\alpha\beta$, 14(3). This is almost the statistical ratio. Although the details of the mechanism and effect of 2Mim or other ligands on the atropisomerization is forthcoming, the effect must be due to the interaction through 2Mim coordinated to ZnToCNPP. This is a novel control of the rotational isomerization by the steric effect of the axial ligand. By this axial ligand effect, the distribution ratio is controlled in the favor of the $\alpha\alpha\alpha\alpha$-form.

We thank the Ministry of Education, Science, and Culture of Japan for support of the part of this work under a Grant-in-Aid for Scientific Research (#60571024). We acknowledge the discussions on the crystal structure of ZnToCNPP(Py)·Py with Professor W. R. Scheidt.

References

1) D. K. Geiger and W. R. Scheidt, *Inorg. Chem.*, **23**, 1970 (1984).

2) F. A. Walker, M.-W. Lo, and M. T. Ree, *J. Am. Chem. Soc.*, **98**, 5552 (1976).

3) V. L. Balke, F. A. Walker, and J. T. West, *J. Am. Chem. Soc.*, **107**, 1226 (1985).

4) a) J. P. Collman, R. R. Gagne, C. A. Reed, T. R. Halbert, G. Lang, and W. T. Robinson, *J. Am. Chem. Soc.*, **97**, 1427 (1975); b) G. B. Jameson, G. A. Rodley, W. T. Robinson, R. R. Gagne, C. A. Reed, and J. P. Collman, *Inorg. Chem.*, **17**, 850 (1978); c) G. B. Jameson, F. S. Molinaro, J. A. Ibers, J. P. Collman, J. I. Brauman, E. Rose, and K. S. Suslick, *J. Am. Chem. Soc.*, **102**, 3224 (1980); d) J. P. Collman, J. I. Brauman, B. L. Iverson, J. L. Sessler, R. M. Morris, and Q. H. Gibson, *J. Am. Chem. Soc.*, **105**, 3052 (1983).

5) D. Lexa, M. Momenteau, P. Rentien, G. Rytz, J.-M. Saveant, and F. Xu, *J. Am. Chem. Soc.*, **106**, 4755 (1984).

6) K. M. More, G. R. Eaton, and S. S. Eaton, *Inorg. Chem.*, **24**, 3698 (1985).

7) a) K. Anzai and K. Hatano, *Chem. Pharm. Bull.*, **32**, 1273 (1984); b) *Idem, ibid.*, **32**, 2067 (1984); c) K. Anzai, T. Hosokawa, and K. Hatano, *ibid.*, **34**, 1865 (1986).

8) a) K. Hatano, K. Anzai, T. Kubo, and S. Tamai, *Bull. Chem. Soc. Jpn.*, **56**, 422 (1983); b) K. Hatano, K. Anzai, A. Nishino, and K. Fujii, *ibid.*, **58**, 3653 (1985).

9) Abbreviations: DMF, *N,N*-dimethylformamide; ToCNPP, 5,10,15,20-tetrakis(*o*-cyanophenyl)porphyrin dianion; ToNH_2PP, 5,10,15,20-tetrakis(*o*-aminophenyl)-porphyrin dianion; ToOHPP, 5,10,15,20-tetrakis(*o*-hydroxyphenyl)porphyrin dianion; TPyP, tetra-4-pyridylporphyrin dianion; TPP side arm Py, 5-[2-[2-(3-pyridyl)ethylcarbonylamino]phenyl]-10,15,20-triphenylporphyrin dianion; OEP, octaethylporphyrin dianion; TPP, tetraphenylporphyrin dianion; Py, pyridine; 2Mim, 2-methylimidazole; N_{por}, porphinato nitrogen atom. N_X, a nitrogen atom belonging to X (X generally denotes a molecule or a group of atoms.).

10) L. K. Gottwald and E. F. Ullman, *Tetrahedron Lett.*, **1969**, 3071.

11) The programs used in this study included local versions and modifications of Sakurai's KFR-5, Okaya and Ashida's XNBLS and FMLS, and Johnson's ORTEP2.

12) Table Sl(listings of the observed and calculated structure amplitudes (×10, 13 pages)), Table S2 (anisotropic temperature factors), and Table S3 (individual bond distances and angles) are deposited as Document No. 8732 at the office of this Bulletin.

13) We use two kinds of estimated standard deviations (esd) in this report. The esd's of the individual positional, thermal, and bond parameters come from the least-squares treatment, i.e., the statistics of F_o and F_c. The other derives from the average statistical treatment of several *chemically equivalent* parameters.

14) D. L. Cullen and E. F. Meyer, Jr., *Acta Crystallogr., Sect B*, **32**, (1976).

15) M. D. Glick, G. H. Cohen, and J. L. Hoard, *J. Am. Chem. Soc.*, **89**, 1996 (1967).

16) D. M. Collins and J. L. Hoard, *J. Am. Chem. Soc.*, **92**, 3761 (1970).

17) M. A. Bobrik and F. A. Walker, *Inorg. Chem.*, **19**, 3383 (1980).

18) a) D. M. Collins, R. Countryman, and J. L. Hoard, *J. Am. Chem. Soc.*, **94**, 2066 (1972); b) J. L. Hoard, in "Porphyrins and Metallopophyrins," ed by K. M. Smith, Elsevier, Amsterdam (1975), pp. 317—380.

19) a) W. R. Scheidt, D. K. Geiger, R. G. Hayes, and G. Lang, *J. Am. Chem. Soc.*, **105**, 2625 (1983); b) D. K. Geiger, V. Chunplang, and W. R. Scheidt, *Inorg. Chem.*, **24**, 4736 (1985).

20) C. K. Schauer, O. P. Anderson, S. S. Eaton, and G. R. Eaton, *Inorg. Chem.*, **24**, 4082 (1985).

21) W. R. Scheidt, D. K. Geiger, Y. J. Lee, C. A. Reed, and G. Lang, *J. Am. Chem. Soc.*, **107**, 5693 (1985).

22) a) P. G. Fauvet, M. Massaux, and R. Chevalier, *Acta Crystallogr., Sect B*, **34**, 1376 (1978); b) I. W. Bassi, C. Benedicenti, M. Calcaterra, and G. Rucci, *J. Organomet. Chem.*, **117**, 285 (1976).

23) D. A. Summerville, I. A. Cohen, K. Hatano, and W. R. Scheidt, *Inorg. Chem.*, **17**, 2906 (1978), and the references cited therein.

24) a) A. Hybl, R. E. Rundle, and D. E. Williams, *J. Am. Chem. Soc.*, **87**, 2779 (1965); b) K. Harata, *Bull. Chem. Soc. Jpn.*, **48**, 2409 (1975).

25) a) K. Odashima, A. Itai, Y. Iitaka, and K. Koga, *J. Am. Chem. Soc.*, **102**, 2504 (1980); b) I. Tabushi, K. Yamanaka, H. Nonoguchi, K. Hirotsu, and T. Higuchi, *J. Am. Chem. Soc.*, **106**, 2621 (1984).

26) F. A. Freitag, J. A. Mercer-Smith, and D. G. Whitten, *J. Am. Chem. Soc.*, **103**, 1226 (1981).

27) E. B. Fleisher, C. K. Miller, and L. E. Webb, *J. Am. Chem. Soc.*, **86**, 2342 (1964).

28) W. R. Scheidt, M. E. Kastner, and K. Hatano, *Inorg. Chem.*, **17**, 706 (1978).

29) W. R. Scheidt, in "The Porphyrins," ed by D. Dolphin, Academic Press, New York (1978), Vol. III, pp. 463—511.